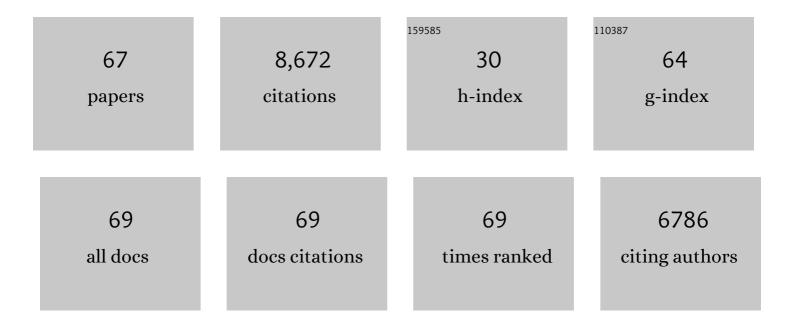
## See-Hun Yang

List of Publications by Year in descending order

Source: https://exaly.com/author-pdf/1958058/publications.pdf Version: 2024-02-01



#	Article	IF	CITATIONS
1	Giant tunnelling magnetoresistance at room temperature with MgO (100) tunnel barriers. Nature Materials, 2004, 3, 862-867.	27.5	2,820
2	Chiral spin torque at magnetic domain walls. Nature Nanotechnology, 2013, 8, 527-533.	31.5	1,029
3	Memory on the racetrack. Nature Nanotechnology, 2015, 10, 195-198.	31.5	644
4	Domain-wall velocities of up to 750â€mâ€sâ^'1 driven by exchange-coupling torque in synthetic antiferromagnets. Nature Nanotechnology, 2015, 10, 221-226.	31.5	548
5	Role of transparency of platinum–ferromagnet interfaces in determining the intrinsic magnitude of the spin Hall effect. Nature Physics, 2015, 11, 496-502.	16.7	465
6	Separation of enantiomers by their enantiospecific interaction with achiral magnetic substrates. Science, 2018, 360, 1331-1334.	12.6	283
7	Enhanced spin–orbit torques by oxygen incorporation in tungsten films. Nature Communications, 2016, 7, 10644.	12.8	266
8	Roadmap of Spin–Orbit Torques. IEEE Transactions on Magnetics, 2021, 57, 1-39.	2.1	225
9	Chiral spin torque arising from proximity-induced magnetization. Nature Communications, 2014, 5, 3910.	12.8	203
10	Chiral spintronics. Nature Reviews Physics, 2021, 3, 328-343.	26.6	191
11	Giant facet-dependent spin-orbit torque and spin Hall conductivity in the triangular antiferromagnet IrMn <sub>3</sub> . Science Advances, 2016, 2, e1600759.	10.3	188
12	Magnetization switching in ferromagnets by adsorbed chiral molecules without current or external magnetic field. Nature Communications, 2017, 8, 14567.	12.8	132
13	Experimental Investigation of Temperature-Dependent Gilbert Damping in Permalloy Thin Films. Scientific Reports, 2016, 6, 22890.	3.3	120
14	Enhanced interface perpendicular magnetic anisotropy in Ta CoFeB MgO using nitrogen doped Ta underlayers. Applied Physics Letters, 2013, 102, .	3.3	117
15	Domain wall trajectory determined by its fractional topological edge defects. Nature Physics, 2013, 9, 505-511.	16.7	112
16	Extremely long quasiparticle spin lifetimes in superconducting aluminium using MgO tunnel spin injectors. Nature Materials, 2010, 9, 586-593.	27.5	102
17	Bias Voltage Dependence of Tunneling Anisotropic Magnetoresistance in Magnetic Tunnel Junctions with MgO and <mml:math <br="" xmlns:mml="http://www.w3.org/1998/Math/MathML">display="inline"&gt;<mml:msub><mml:mi>Al</mml:mi><mml:mn>2</mml:mn></mml:msub><mml:msub><mml:mi mathvariant="normal"&gt;O<mml:mn>3</mml:mn></mml:mi </mml:msub></mml:math> Tunnel Barriers.	7.8	98
18	Physical Review Letters, 2007, 99, 226602. Current Induced Tilting of Domain Walls in High Velocity Motion along Perpendicularly Magnetized Micron-Sized Co/Ni/Co Racetracks. Applied Physics Express, 2012, 5, 093006.	2.4	93

#	Article	IF	CITATIONS
19	Exchange coupling torque in ferrimagnetic Co/Gd bilayer maximized near angular momentum compensation temperature. Nature Communications, 2018, 9, 4984.	12.8	78
20	Observation of the intrinsic Gilbert damping constant in Co/Ni multilayers independent of the stack number with perpendicular anisotropy. Applied Physics Letters, 2013, 102, .	3.3	69
21	Giant thermal spin-torque–assisted magnetic tunnel junction switching. Proceedings of the National Academy of Sciences of the United States of America, 2015, 112, 6585-6590.	7.1	59
22	Crossover from Kondo-Assisted Suppression to Co-Tunneling Enhancement of Tunneling Magnetoresistance via Ferromagnetic Nanodots in MgO Tunnel Barriers. Nano Letters, 2008, 8, 340-344.	9.1	57
23	Domain wall memory: Physics, materials, and devices. Physics Reports, 2022, 958, 1-35.	25.6	56
24	Determination of intrinsic damping of perpendicularly magnetized ultrathin films from time-resolved precessional magnetization measurements. Physical Review B, 2015, 92, .	3.2	54
25	Dramatic influence of curvature of nanowire on chiral domain wall velocity. Science Advances, 2017, 3, e1602804.	10.3	42
26	Spintronics on chiral objects. Applied Physics Letters, 2020, 116, .	3.3	39
27	Chiral domain wall motion in unit-cell thick perpendicularly magnetized Heusler films prepared by chemical templating. Nature Communications, 2018, 9, 4653.	12.8	35
28	Probing buried interfaces with soft x-ray standing wave spectroscopy: application to the Fe/Cr interface. Journal of Physics Condensed Matter, 2002, 14, L407-L420.	1.8	34
29	Highly Efficient In-Line Magnetic Domain Wall Injector. Nano Letters, 2015, 15, 835-841.	9.1	32
30	Determination of layer-resolved composition, magnetization, and electronic structure of an Fe/MgO tunnel junction by standing-wave core and valence photoemission. Physical Review B, 2011, 84, .	3.2	31
31	CoFe alloy as middle layer for strong spin dependent quantum well resonant tunneling in MgO double barrier magnetic tunnel junctions. Physical Review B, 2013, 87, .	3.2	30
32	Negative Tunneling Magnetoresistance by Canted Magnetization in <mml:math xmlns:mml="http://www.w3.org/1998/Math/MathML" display="inline"&gt;<mml:mi>MgO</mml:mi><mml:mo>/</mml:mo><mml:mi>NiO</mml:mi>Tunnel Barriers. Physical Review Letters, 2011, 106, 167201.</mml:math 	7.8	28
33	Novel domain wall dynamics in synthetic antiferromagnets. Journal of Physics Condensed Matter, 2017, 29, 303001.	1.8	27
34	Nonlinear Magnetization Dynamics Driven by Strong Terahertz Fields. Physical Review Letters, 2019, 123, 197204.	7.8	26
35	Setting of the magnetic structure of chiral kagome antiferromagnets by a seeded spin-orbit torque. Science Advances, 2022, 8, .	10.3	25
36	Chiral exchange drag and chirality oscillations in synthetic antiferromagnets. Nature Physics, 2019, 15, 543-548.	16.7	23

#	Article	IF	CITATIONS
37	The role of Mg interface layer in MgO magnetic tunnel junctions with CoFe and CoFeB electrodes. AIP Advances, 2012, 2, .	1.3	21
38	Highly Asymmetric Chiral Domain-Wall Velocities in Y-Shaped Junctions. Nano Letters, 2018, 18, 1826-1830.	9.1	21
39	Increased Tunneling Magnetoresistance Using Normally bcc CoFe Alloy Electrodes Made Amorphous without Glass Forming Additives. Physical Review Letters, 2009, 102, 247205.	7.8	19
40	Coexistence of the Kondo effect and a ferromagnetic phase in magnetic tunnel junctions. Physical Review B, 2011, 83, .	3.2	19
41	X-ray studies of interface Fe-oxide in annealed MgO based magnetic tunneling junctions. Journal of Electron Spectroscopy and Related Phenomena, 2012, 185, 133-139.	1.7	19
42	lonitronic manipulation of current-induced domain wall motion in synthetic antiferromagnets. Nature Communications, 2021, 12, 5002.	12.8	18
43	Bias dependence of spin transfer torque in Co2MnSi Heusler alloy based magnetic tunnel junctions. Applied Physics Letters, 2017, 110, .	3.3	15
44	Phase-resolved detection of the spin Hall angle by optical ferromagnetic resonance in perpendicularly magnetized thin films. Physical Review B, 2017, 95, .	3.2	13
45	Increased Efficiency of Currentâ€Induced Motion of Chiral Domain Walls by Interface Engineering. Advanced Materials, 2021, 33, 2007991.	21.0	13
46	Robust sorting of chiral domain walls in a racetrack biplexer. Applied Physics Letters, 2014, 105, 222404.	3.3	12
47	High-resolution Ce3dâ~'edgeresonant photoemission study ofCeNi2. Physical Review B, 2000, 61, R13329-R13332.	3.2	11
48	High-Resolution Photoemission Study of UNi2Al3and URu2Si2. Journal of the Physical Society of Japan, 1996, 65, 2685-2689.	1.6	10
49	Tunneling spin polarization measurements from ferromagnet/MgO tunnel junctions using NbN superconductor. Applied Physics Letters, 2006, 88, 182501.	3.3	10
50	Optimized thickness of superconducting aluminum electrodes for measurement of spin polarization with MgO tunnel barriers. Applied Physics Letters, 2007, 90, 202502.	3.3	10
51	Giant Spin Hall Effect and Spin–Orbit Torques in 5 <i>d</i> Transition Metal–Aluminum Alloys from Extrinsic Scattering. Advanced Materials, 2022, 34, e2109406.	21.0	10
52	Current driven chiral domain wall motions in synthetic antiferromagnets with Co/Rh/Co. Journal of Applied Physics, 2020, 128, 053902.	2.5	9
53	Giant oscillatory Gilbert damping in superconductor/ferromagnet/superconductor junctions. Science Advances, 2021, 7, eabh3686.	10.3	9
54	Experimentally tunable chiral spin transfer torque in domain wall motion. New Journal of Physics, 2016, 18, 053027.	2.9	8

#	Article	IF	CITATIONS
55	Asymmetric magnetic disorder observed in thermally activated magnetization reversal of exchange-biased IrMn/CoFe films. Journal of Magnetism and Magnetic Materials, 2013, 325, 13-16.	2.3	7
56	An all-electrical magnetic logic gate that harnesses chirality between domains. Nature, 2020, 579, 201-202.	27.8	6
57	Surface and bulk4fphotoemission spectra ofCeIr2. Physical Review B, 1999, 59, 12294-12297.	3.2	5
58	Spin-Orbit Torque Driven One-Bit Magnetic Racetrack Devices - Memory and Neuromorphic Applications. , 2019, , .		5
59	Role of Micromagnetic States on Spin–Orbit Torque-Switching Schemes. Nano Letters, 2018, 18, 4074-4080.	9.1	4
60	Chirality tweaks spins in tellurium. Nature Materials, 2022, 21, 494-495.	27.5	4
61	Efficient Chiral-Domain-Wall Motion Driven by Spin-Orbit Torque in Metastable Platinum Films. Physical Review Applied, 2020, 14, .	3.8	3
62	Interplay between superconductivity and the Kondo effect on magnetic nanodots. Applied Physics Letters, 2021, 118, 152407.	3.3	3
63	Half-integer Shapiro steps in strong ferromagnetic Josephson junctions. Physical Review B, 2021, 104, .	3.2	3
64	Resonant Enhancement of Exchange Coupling for Voltage-Controlled Magnetic Switching. Physical Review Applied, 2020, 14, .	3.8	2
65	Determination of the spin Hall angle by the inverse spin Hall effect, device level ferromagnetic resonance, and spin torque ferromagnetic resonance: A comparison of methods. Applied Physics Letters, 2021, 119, .	3.3	2
66	Effect of microstructures on the Gilbert damping in Co/Ni multilayers. Current Applied Physics, 2016, 16, 1349-1352.	2.4	0
67	Perpendicular Exchange Bias of CoNi Multilayers Interfacing with Antiferromagnetic IrMn Layer. Journal of the Korean Magnetics Society, 2017, 27, 210-214.	0.0	0